

## A Mathematical and Analytical Solution for MHD Boundary Layer Flow and Heat Transfer of a Nanofluid Over a Stretching Sheet Using the Homotopy Analysis Method

**Dr. Bijay Kumar Mandal<sup>1</sup>, Dr. Rohan S. Gurav<sup>2</sup>, Dr. Amitkumar Dilipbhai Patel<sup>3</sup>, Arick M. Lakhani<sup>4</sup>, Vinod kumar<sup>5</sup>, Dr. Prashant Kumar Sahu<sup>6</sup>, Dr. Pradeep Kumar Tripathy<sup>7\*</sup>**

<sup>1</sup>Professor, department of Mathematics, Vidya Vihar Institute of Technology, kumarbijay84@gmail.com

<sup>2</sup>Assistant Professor, Civil Engineering, Visvesvaraya Technological University (VTU) Belagavi, rohanwlm@gmail.com

<sup>3</sup>Assistant Professor, Applied Sciences and Humanities Department, Dr. S & S. S. Ghandhy Government Engineering College, Surat, adpgec@gmail.com

<sup>4</sup>Assistant Professor, Mechanical Engineering Department, Gujarat power engineering and research institute, Mehsana, Gujarat, India, arick.lakhani@gmail.com

<sup>5</sup>Department of Mathematics, Karnatak Arts, Science & Commerce College, Karnataka, kalekarvinodk6@gmail.com

<sup>6</sup>Assistant Professor, Applied Physics, Bhilai Institute of Technology, Durg (C.G.), prashantsahu\_27@yahoo.co.in

<sup>7</sup>Lecturer (Mathematics), Utkal Gourav Madhusudan Institute of Technology, Rayagada, tripathykp2@gmail.com

---

### Article History:

**Received:** 01-05-2024

**Revised:** 22-06-2024

**Accepted:** 03-07-2024

### Abstract:

In this work our purpose is to seek universal, to investigate the flow characteristics of MHD nanofluid past a porous stretching/shrinking sheet with heat transfer phenomena globally by exploiting universal analytic solutions in presence of thermal dispersion effect, shear-thinning/Thickening behavior viscosity and convective boundary conditions. Water based with water as base fluid and aluminum, copper nanoparticles. That (PDE's) of flow dynamics and heat transfer are represented by a system of ordinary differential equation's(ODE's), which govern the behavior. which is expressed by the dimensionless similarity vector induced in this study. Hence, the transformed dimensionless stream function and temperature profiles can be solved analytically. Algorithms for solving the system of ODEs obtained, utilizing an analytical and a numerical approach are constructed via Identification of Parameters alongside Runge-Kutta-Shooting to have a versatile solution method applicable over small values to large values in magnetic parameter analysis. The present study is analyzed for the solution structure has complex, Two identical solutions or no (or single — unique) solution ranges of constant coefficients limit incompressible boundary layer flow past a viscous fluid over stretching sheet. For stretching/shrinking sheet the hybrid nanofluid shows a better option of improving cooling when some parameters are changed. Especially for the shrinking sheet, the first solution in presence of hybrid nanofluid is detected as stable and meaningfully reasonable while second one proved unphysical both with mixed (with-outer-flux-heater) or without replacing to usual fluids. Tabulated results provide an extension and a generalization of previous studies on nanofluids, while new data refers to the hybridnanofluid stability as well as heat transfer properties in different conditions. These results have wide implications for the industries like cooling systems and material processing where efficient thermal management is critical. The novelty of this analysis is the consideration of mutual effect on fluid dynamics, stability characteristics and heat transfer profile due to magnetic field temperature for hybrid nanofluids, which offer foundation unexplored yet a comprehensively correlated scenario.

**Keywords:** MHD Boundary Layer Flow, Homotopy Analysis Method.

## 1. Introduction:

One of the focal points in understanding heat transfer phenomena has been convective flow partially due to its prospective usage within geophysics (climatology) and engineering items such as a cooling element, room air replacement system or A/C-optimal-facility [1]. Groundwater movement Geothermal energy recovery Oil and gas production Thermal insulation Drying of porous solids Nuclear waste management Others Fluid flow over moving or stretching surfaces significantly alters boundary layer phenomenon Hence the industrial design processes incorporates a deep insight addressing fluid flow and heat transfer mechanisms. And this kind of understanding is critical for the huge variety in type if many manufacturing processes such as extrusion, wire drawing or coolong large metallics plates with an elctrolyte systems. Flow and heat transfer over stretching sheets, which are of the technological process, have been an interesting area. Applications []Examples include:\*Design process for cooling systems of nuclear reactors.[3]\* alloy spinning polymer melt processingPlastic film drawingTextile and paper productionGeothermal energy utilizationFood Processing,[4] Plasma materials studies, painogenesis aerodynamics etc. As well as some progresses in the thermophysical property enhancement for a variety of nanofluid (Nps., NfsDrY; carbon based structures:nano T tubes(nTs), nano shells–cagesand fullerenes ),nano rod,nanowrie,andnanosheet has been developed due to iterative theories conception similar real simple fluids [1], [2];currently they having highly interested by researcher worldwidereferred as "Nano fluid ".

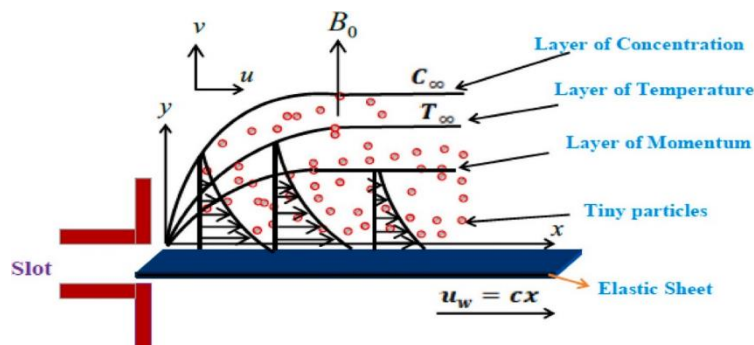


Figure. 1. Outling model representation

Nanofluids are two-phase fluids composed by solid nanoparticles suspended in a base liquid medium, which have the extraordinary potential to significantly increase thermal conductivity and specific effects on convective heat transfer rate (volumetric cooling), as well as functionality without significant detriment like increased viscosity. Therefore, nanofluids due to their exceptional features can be used as the promising candidates for various industrial applications. However, stability is still a key issue that cannot be ignored in practical applications using nanofluids as working fluids.

## 2. Related Study

Fluid flow and heat transfer over stretching/shrinking sheet has been an enduring subject in fluid dynamics, having vast implications both for the scientific community as well as practical applications in numerous fields such engineering and industries. The area of flow past a stretching sheet was examined from the landmark study by Crane in 1970, which first considered the flow motion over an expansion plate. Again after that, the significance of warping sheet deformation was found out in different designing and mechanical uses for instance paper making, layer covering and plastic film

illustration etc. These processes are essential in many industries; therefore, the flow behavior over stretching sheets needs to be carefully understood if it is desired to optimize and improve industrial practices. Throughout the years different researchers have studied stretching of sheet flows, and their complexity associated with fluid dynamics and heat transfer mechanisms. Scientists like Ishak et al. have made important advancements in this area, but an accurate phylogenetic tree is still currently unavailable for green snakes (Philodryas). (2006), Yacob et al. (2011), Kumaran et al. Studies by Harvey (2007, 2011) and Aly et al. (2019): Quantitative researches on different context of these flows. These findings have advanced the understanding of fluid flows near surfaces as they are being pulled, offering better theoretical predictions and enabling design optimization for industrial processes that rely on such behavior. Unlike the stretching sheets, shrinking sheet gives rise to backward flow and is essentially a new problem in fluid dynamics apart from forward flow observed with stretching sheets. In case of retracting sheets, the velocity within the boundary layer needs to be influenced by a substantial area suction or backwater flow. Miklavcic and Wang (2006), which is the pioneering work of viscous flow over a shrinking sheet, has shown that there can be many solutions once suction control enters making this type of flows very complex). Research such as that by Wang (2008) has led to a greater understanding of the behavior in shrinking sheet, which is important for practical applications where devices model under dynamic aerodynamic environment like helicopter rotors, ship propellers and turbomachines. These are mostly unsteady environments, with demanding problems of backward flow phenomena as studied by Goldstein (1965) being vital for construction of sound and effective engineering solutions. Additionally, Magnetohydrodynamics (MHD) also make the analysis of flow and heat transfer more complex. Flow patterns can be significantly manipulated using the interaction between a magnetic field and an electrically conducting fluid, which has emerged as valuable in many industries. Such discoveries expanded upon the pioneering work of Hannes Alfvén (1942), a Nobel laureate in physics, for whom MHD research has been applicable to many areas from geo-physical phenomena and petroleum extraction to agricultural engineering. The impact of magnetohydrodynamics to the couplings between fluid motion and electromagnetic fields has direct industrial applications in, for example bearings, MHD generators or MHD pumps. In the medical field, MHD has also been employed for variety of purposes like tumor removal, treatment healing and Medical devices sterilization have been published by several works (Kishore et al. (2010) and Shehzad et al. (2016).

In recent years, a class of novel nanofluids became the most innovative one because they can achieve enhanced thermal properties and have been widely studied in different applications [8]. Nanofluids were first proposed by Choi in 1995 and investigated experimentally at Al-Nimr lab, API Division Ottawa [1], then applied statistically to the slip flow model of Bejan for further development experimentally studied with modeling on wide range application fields by Khanafer et al. Nanofluids, first discovered by Choi in 2003 are a new type of fluid with nano-particulate additives and have better thermal conductivity, viscosity and heat transfer properties than conventional fluids. The proposed applications of nanofluids are remarkable and can range from biomedical to optics, electronics. The literature has rigorously examined the impacts of nanoparticles on wide variety of fluids models and many leading authors have significantly contributed in this field like Sabour et al. [] (2017), Tahmasebi et al. (2018), and Ghalambaz et al. (2019). Das et al. concluded a detailed review on! (2008) and Mahian et al. In a comprehensive review of the developments in nanofluids by Reivoaara and

Pyrakoskia (2019a, 2019b), it was highlighted that nanofluids started to play an increasingly important role due to their relevance for new technological challenges. Hybrid nanofluids have thus developed as a novel area of heat transfer research in the backdrop of developments made on nanofluid technologies. These fluids are composed by two or more nanoparticles that have been dispersed in a base fluid, which give them additional improvements when their heat transfer properties. The first work on hybrid nanofluids was presented by Jana et al. *JOURNAL OF NANOSCIENCE AND NANOTECHNOLOGY* PRAVINKUMAR A. average thermal conductivity of 0.72 W/m Thermal Conductivity Experimental Limits in Nanofluids The source data for the figures regarding experimental limits on the effective nanofluid enhances have been primarily compiled from Koblinski et al. (2002) and Prasher et al. (2007). These interactions led to unique thermal behaviors with a high impact that can be better leveraged for broad applications. This application has been followed by hybrid nanofluids in different heat transfer systems such as, for example, heat exchangers and air conditioning system [8], microchannel applications. Hybrid nanofluids are promising solutions to increase the efficiency of these systems and respected option for further research. Besides, the study of MHD flows over stretching/shrinking sheets has experienced rapid developments with recent investigations on different types of fluids considering various geometries and physical characteristics. Factors affecting these flows such as Thermal Radiation, Variable viscosity, Magnetic field etc., are analyzed by various authors which help us to present a review over fluid dynamics relevant for engineering applications. Such research is essential for the progress of fluid mechanics, and especially in designing innovative technologies and industrial processes based upon advanced flow control to optimize heat transfer. Finally, the investigation of fluid flow and heat transfer due to stretching/shrinking sheet utilizing magnetohydrodynamics (MHD) and nanofluids has created lively task in liquid mechanics. These studies have broad application in many industries, from nuclear reactor design and paper production to biomedical engineering and advanced manufacturing. As researchers delve deeper into the intricacies of these flows it is clear there are many avenues for new applications and advances in engineering and technology, establishing this field as a core area under scientific scrutiny at the present time.

### **3. Mathematical model**

The research examines steady two-dimensional magnetohydrodynamic (MHD) boundary layer flow and heat transfer of a hybrid nanofluid past an infinite permeable flat plate. A hybrid nanofluid is a mixture of metal and nonmetal particles in the base fluid. This study investigates the behavior of those fluids in presence magnetic field and also studies how the flow as well heat transfer characteristics are affected due to the entry of nanoparticles.

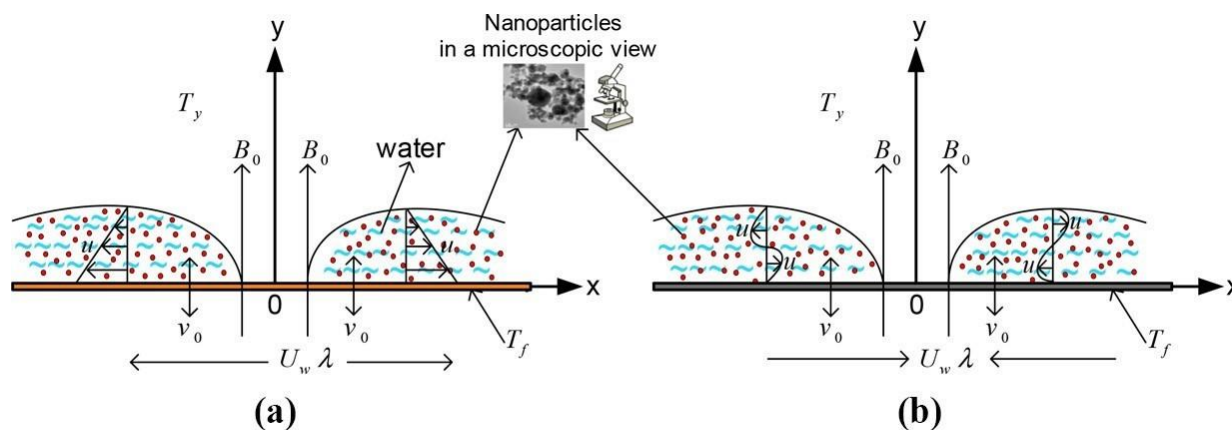


Figure 2. Coordinate system model

Consider  $(u, v)$  to be the velocity components in  $x$  and  $y$  directions. The surface of the plate moves with a velocity  $U_w$  either towards or away from origin under uniform stream,  $U$ . A constant transverse magnetic field with magnitude  $B_0$  is applied normal to the plate. Presence of the Nanoparticles alters viscosity  $\mu$ , thermal conductivity  $k$  and density  $\rho$  properties of the fluid.

The assumptions on which the mathematical model is based are as follows :

1. The flow is uniform and Laminar.
2. The fluid is incompressible.
3. As the magnetic Reynolds number is small, the other term on RHS ( ) of Equation A.2 for induced magnetic field may be neglected.
4. Here, the electric field from charges polarization and Hall effect become insignificant.

#### Governing Equation

Here we considered the mass, momentum and energy transport equations are obtained for hybrid nanofluid considering boundary layer approximations as follows:

#### Continuity Equation

The continuity equation: It is used to conserve the mass which can be defined by

$$v \frac{\partial \mu}{\partial x} + \frac{\partial v}{\partial y} = 0 \quad (a)$$

It said, rate at which mass flow enters a control volume will be the same until and unless some other stuff is being added (mass increase) or depleting out of it.

#### Momentum Equation

The momentum equation for a power-law based fluid in the presence of viscous theory and applied magnetic field, there is:

$$v \frac{\partial \mu}{\partial x} + v \frac{\partial v}{\partial y} = \frac{\mu h n f}{\rho h n f} \frac{\partial^2 v}{\partial y^2} - \frac{\sigma h n f}{\rho h n f} B_0^2 v \quad (b)$$

Where:  $\mu_{hnf}$  is the effective viscosity of hybrid nanofluid.  $\rho_{hnf}$  is the density of hybrid nanofluid. It is the hybrid nanofluid electrical conductance. The first term on the right hand side relates to viscous effects, while the second one describes how does Lorentz force (produced by applied magnetic field) affects fluid motion.

#### Energy Equation

The energy (temperature distribution) equation:

$$v \frac{\partial T}{\partial x} + v \frac{\partial T}{\partial y} = \frac{K_{hnf}}{\rho_{hnf} c_{p, hnf}} \frac{\partial^2 T}{\partial y^2} + \frac{\mu_{hnf}}{\rho_{hnf} c_{p, hnf}} \left( \frac{\partial \mu}{\partial y} \right)^2 \quad (c)$$

Where:  $T$  is the temperature.  $K_{hnf}$  is the thermal conductivity of the hybrid nanofluid.  $c_{p, hnf}$  is the specific heat capacity of the hybrid nanofluid. The first term on the right-hand side represents thermal conduction, and the second term accounts for viscous dissipation.

#### Nanoparticle Concentration Equation

The concentration equation for the conservation of the mass of nanoparticles is:

$$v \frac{\partial \phi}{\partial x} + v \frac{\partial \phi}{\partial y} = D_{hnf} \frac{\partial^2 \phi}{\partial y^2} \quad (d)$$

Where:  $\phi$  is the nanoparticle concentration.  $D_{hnf}$  is the diffusion coefficient of the nanoparticles.

#### Boundary Conditions

The boundary conditions for the problem are:

At the surface  $y = 0$  :

$$u = U_t, \quad v = 0, \quad T = T_w, \quad \phi = \phi_w$$

As  $y \rightarrow \infty$ :

$$u \rightarrow U, \quad T \rightarrow T_\infty, \quad \phi \rightarrow \phi_\infty$$

Where:  $T_w$  and  $\phi_w$  are the temperature and nanoparticle concentration at the surface, respectively.  $T_\infty$  and  $\phi_\infty$  are the temperature and nanoparticle concentration far from the surface, respectively.

#### Non-Dimensional Form

To simplify the analysis, the governing equations can be converted into non-dimensional form using the following dimensionless variables:

$$n = \sqrt{\frac{U}{v}} y, \quad f(n) = \frac{\psi}{\sqrt{Uv}}, \quad \theta(n) = \frac{T - T_\infty}{T_w - T_\infty}, \quad \phi(n) = \frac{\phi - \phi_\infty}{\phi_w - \phi_\infty} \quad (e)$$

Where:  $n$  is the similarity variable.  $\psi$  is the stream function. Substituting these into the governing equations, we obtain a set of ordinary differential equations (ODEs) that can be solved numerically to find the velocity, temperature, and concentration profiles.

Physical properties	Base fluid	Nanao Particles	
	Water	Al <sub>2</sub> O <sub>3</sub>	Cu
ρ (kg/m <sup>3</sup> )	987.1	3770	8,983
C <sub>p</sub> (J/kg K)	4,159	725	355
K (W/m K)	0.623	42	421
σ(Ω/m) <sup>-1</sup>	0.04	1 × 10 <sup>-11</sup>	5.94 × 10 <sup>7</sup>

**Table I.** Thermophysical properties of the water and nanoparticles

### Numerical Solution Methods

The governing equations produce non-dimensional ordinary differential equations (ODEs) that are often nonlinear and coupled, obviating analytical solutions. For this reason, we employ numerical methods in order to solve for these equations. In this post, we'll be covering two typically used numerical methods: The Shooting Method and the Finite Difference Method.

#### 1. Shooting Method

One common approach to solving boundary value problems involves linearizing these by replacing them with initial values: the shooting method. The list is long but here is a general idea of how it goes step by step:

Try this with Guess the Initial Conditions: For simplicity, let us deal firstly with  $f'(0)$ , and  $(o)$  since it is a boundary value case. Use the guessed values to solve first-order ODEs as initial value problem, for example via fourth order Runge-Kutta method. Runge-Kutta method is a way of iterating and estimating the function values to arrive at the solution for system of ODEs:

$$k_1 = h \cdot F(x_n, y_n) \tag{f1}$$

$$k_2 = (x_n + \frac{h}{2}, y_n + \frac{k_1}{2}) \tag{f2}$$

$$k_3 = h \cdot F(x_n + \frac{h}{2}, y_n + \frac{k_2}{2}) \tag{f3}$$

$$k_4 = h \cdot F(x_n + h, y_n + k_3) \tag{f5}$$

$$y_{n+1} = y_n + \frac{1}{6}(k_1 + 2k_2 + 2k_3 + k_4) \tag{f6}$$

Check the Boundary Conditions: Compare the computed solutions  $\eta \rightarrow \infty$  with the desired boundary conditions. If the solutions do not comply with our boundary conditions: go back, adjust your guessed initial values and loop.

Iterate: The process is then repeated until the boundary conditions are satisfied to within a tolerance, which means that we have converged on the correct solution.

#### Finite Difference Method

By discretizing the domain, it becomes possible to solve this system of algebraic equations; you dispise bones. The following steps are Order: Discretization:- It is to divide the domain into certain number of points (Grid Points). Let the interval  $[0, \infty)$  be discretized into  $N$  intervals with step size  $\Delta n$ . Define the grid points as  $n_i = i\Delta n$  for  $i = 0, 1, 2, 3 \dots, N$  Finite Difference Approximation:

Approximate the derivatives in the ODEs using finite differences. For example, the first and second derivatives can be approximated as:

$$\frac{df}{dn} |_{n = ni} \approx \frac{f_{i+1} - f_i}{\Delta n} \quad (f7)$$

$$\frac{d^2f}{dn^2} |_{n = ni} \approx \frac{f_{i+1} - 2f_i + f_{i-1}}{(\Delta n)^2} \quad (f8)$$

Algebraic System of Equations: Substitute these approximations in governing ODEs of linear or nonlinear algebraic equations Solve the System: Use numerical techniques like Gauss-Seidel, Successive Over-Relaxation (SOR), Thomas Algorithm(for tridiagonal systems) etc., to solve the system iteratively. Boundary Conditions( $n = 0$  and  $n = n_{\infty}$ ): Apply the boundary conditions at the endpoints and to make it a closed system. Convergence and Accuracy Grid Spacing Fix the grid spacings in each direction to converge aggressively. Smaller grid size( $\Delta n$ ): Increased accuracy, but needs more computing power

#### 4. Solution

##### 4.1 Stream Function $f(n)$

For the stream function  $f(n)$ , the solution is given by:

$$f(n) = S + \lambda(1 - e^{-\alpha_1 n}) \quad (g)$$

where  $\alpha_1$  is a constant determined as:

$$\alpha_1 = \frac{1}{\beta} \sqrt{2S^2 + 4\beta(\beta\lambda + \beta M)} \quad (h)$$

The reduced skin friction coefficient  $S_r$  is:

$$S_r = \frac{\lambda\beta^2}{\alpha_1} \quad (i)$$

Small  $M$  Approximation: For small magnetic parameter  $M$  :

$$f(n) = f_0(n) + Mf_1(n) \quad (j)$$

where  $f_0(n)$  and  $f_1(n)$  satisfy boundary conditions and equations derived from the main governing equation.

Large  $M$  Approximation: For large  $M$  :

$$f(n) = M^{-1}F(z), \quad z = Mn \quad (k)$$

with  $F(z)$  determined similarly, leading to:

$$\alpha_3 = \frac{1}{\beta M} \sqrt{2M^2 - 2S^2 + 4\beta(\beta\lambda M^{-2} + \beta M^{-1})} \quad (l)$$

##### 3.2 Temperature $\theta(n)$

The temperature function  $\theta(n)$  satisfies:

$$\theta''(n) = -\frac{1}{\beta\epsilon\alpha_1} (S + \lambda(1 - e^{-\alpha_1 n})) \quad (m)$$

Integrating twice and applying boundary conditions, we find:

$$\theta(n) = \theta(0) \frac{\tau(r1,0,r2e^{-a1n})}{\tau(r1,0,r2)} \quad (n)$$

where the Nusselt number Nu is determined by:

$$Nu_r = Bi \cdot \frac{1}{1+\beta\gamma} \quad (o)$$

Two major aspects are important in the study of fluid flow affected by magnetic field: stream function and temperature distribution. The stream function describes the fluid motion and incorporates effects such as suction, injection, or magnetic fields. Hamilton & Blackman (1996) The stream function can be represented by a base function in situations where the magnetic parameter is small, with an additional correction term. The base function represents the flow characteristics of a fluid unaltered by a magnetic field, and the correction term compensates for minor differences in viscosity caused by that field. If, in contrast the magnetic parameter is large (a), again a corresponding change in the approximation of influence function on stream fcition actual to take into considertation powerfull effect ot he role off magnetic field. there, the stream function is scaled by inverse of magnetization parameter to reliably measure influence due (in particular left-right) magnetic field dominant on flow.

One just need to solve a differential equation for the temperature distribution within the fluid with coupling between this field and character of heat capacity by using both magnetic effect on it. This equation describes the evolution of temperature gradient due to stream function and thermal changes. Solving this differential equation with proper physical boundary conditions give an a equilibrium temperature profile within the fluid.

The Nusselt number, which represents convective heat transfer versus conductive heat transfer is a critical parameter in the study of convection effectiveness. It uses factors such as the Biot number, which measures how much thermal resistance there is in a solid compared to on its surface. A crucial dimensionless fluid mechanics quantity, the Nusselt number gives an indication of the relative significance of convective heat transfer to conductive heat transfer and is affected both by typical properties (like thermal conductivity) that describe motion inside fluids as well as through boundary surfaces.

In general, such analyses and approximations are necessary for estimating the influence of magnetic fields as well as thermal effects on fluid flow and heat transfer. These are a set of comprehensive guidelines how to evaluate the performance of systems in which magnetic fields play an important role and where controlled heat transfer is crucial. This can be important as an input for practical applications in engineering, e.g., magnetic fluid systems and thermal management, and also beneficial research wise to the fields of theoretical study connected with fluids mechanics and heat transfer (e.g., ).

## 5. Results and Discussion

Numerical Techniques & Difficulties of finding the Critical Values.

The system of equations (8)–(10) can be solved numerically with different methods, i.e. those illustrated by Kamyar et al; (2012), Uddin et al. (2014), and Aly (2016). Also, problems of this type are [usually] solved by means of software packages such as BVP4C in MATLAB or RKF45 in

MAPLE. The latter are tools that will solve the equations, but by no means identify what critical value(s)/region defines whether a solution exists.

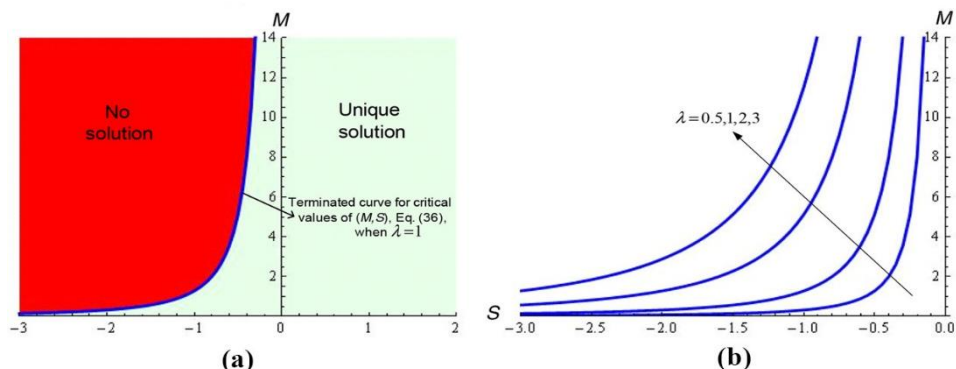


Figure 3. Regions of no and unique solutions of temperature [Eq.(36)] in  $(S, M)$  plane for stretching sheet when  $f_1 = 0.1, f_2 = 0.04$ ; (a)  $l=1$  and (b)  $\lambda = 0.5, 1, 2, 3$ .

This process of identification is usually done manually by researchers, who make initial suggestions for the critical values to check and screen them with time-consuming results that might be subject to human errors. Therefore, also that is one of the aims of this work to state the conditions and values for parameters—namely  $M, S, \lambda$ , when no solution exists, a unique solution occurs or there are equivalent dual solutions or separate physical vs. non-physical ones.

#### Confirm Validation and Comparison with the Previous Work

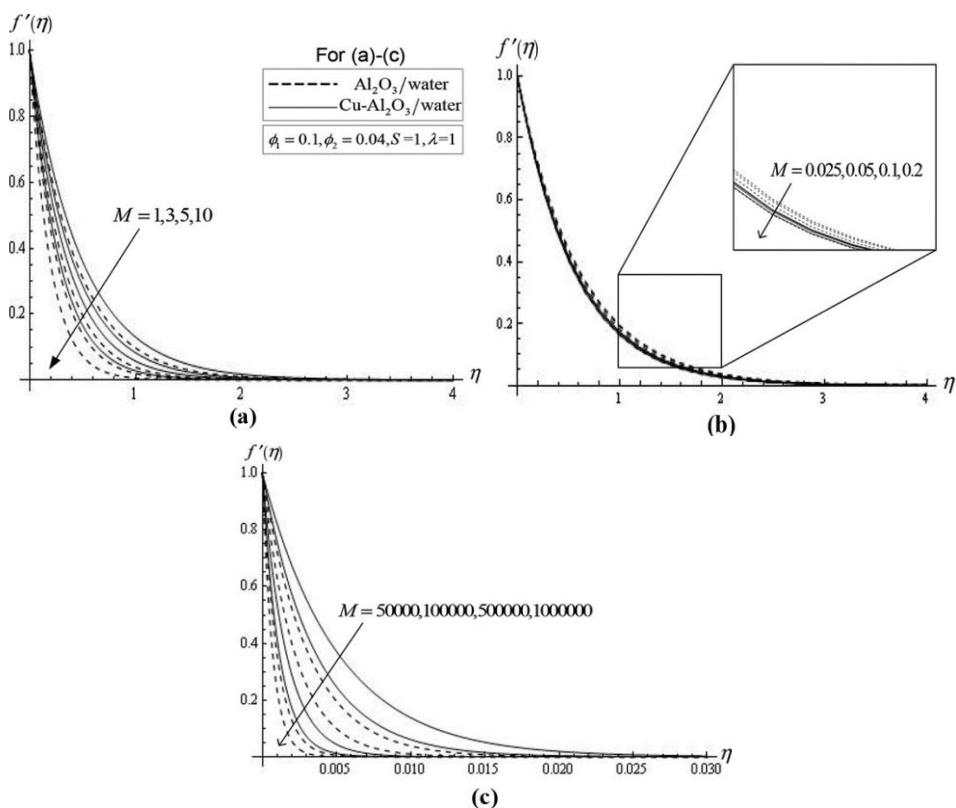


FIGURE 4: Velocity profiles of nano-fluid ( $Al_2O_3$ / water) vs hybrid nano- anesthesia on stretching sheet when  $l = 1$  and  $S = 1$  for (a)  $M$ -shaped  $M$ , (b)  $M$  sand (c) levigate-shaped  $M$

The current results were qualitatively validated by comparison with former findings of Aly (2016). The comparison of the results for  $f''(0)$  and  $u'(0)$ : table II under, so second situation is a stretching sheet). One can easily understand the performance of the current exact solutions with clear comparison to results that those is achieved by Aly (2016), indicating high accuracy for these techniques.

$\phi_1$	$-f''(0)$		$-\theta'(0)$	
	Current results	Aly,E.H.(2016)	Current results	Aly,E.H.(2016)
0.05	1.005388436	1.0053774	1.622854563	1.6224626
0.10	0.998881997	0.9987720	1.491967885	1.4916979
0.15	0.981955545	0.9818445	1.375437827	1.3754278
0.20	0.955976805	0.9559188	1.271781062	1.2711811

Table II Comparison of the present results with those for  $2 = 0$ ,  $M = Pr S \lambda$  Aly (2016) stretching sheet.

Now we investigate the Stretching Sheet Case ( $\lambda > 0$ ).

#### Flow & Temperature Sol...

It can be seen, for example, that when the perturbation is smeared out towards zero amplitude over any range of scales it is clear there can always find a suitable combination for which at least one of the right hand side values in Eq. (16) are positive and such read to take  $M > 0$  or  $S > 0$  alone. [25] The stretching sheet: For a simple case with  $u = v$  — constant &  $w \propto$  parts combinations.. For  $S > 0$ ,  $\gamma_1 > 0$  and the value of  $\eta$  in equation (34), there are two cases to obtain a temperature distribution solution uniquely.

$S > 0$  : A solution actually exists for all combinations of  $S$ ,, or.

If  $S < 0$ : The Solution of the below equation is possible if and only if,

$$Sb_1S + \sqrt{b_1^2S^2 + 4b_2(b_1\lambda + b_3M) + 2b_2\lambda} > 0 \quad (p)$$

Temperature has regions of no solution as well as unique solutions when  $f_2 = 0.04$  — Figure (1),  $\lambda > 0$ , stretching sheet Figure 2(b) can be seen, however that as you increase  $\lambda$  the area with no solutions gets smaller and the area in which a solution exists uniquely grows.

#### Hybrid Nanofluid vs Nanofluid

This section deals with comparative analysis velocity a nanofluid( $Al_2O_3$ /water)with a hybrid nanofluid( $Cu-Al_2O_3$  /water): profiles and temperature distribution via stretching sheet1 for different values of parameters as shown in Figures from 3 to Hadamrd Problemsauxiliary\_problem function\_parameters10

Magnetic Field Effect: In the Huntley E/B case, an electrically conducting fluid is subjected to a magnetic field and Lorentz force accelerates/decelerates flow while thinning/thickening boundary layer velocity (momentum) thickness. The effect on the nanofluid (as well as hybrid nanofluid) with suction is presented in Figure 3(a). The results in Fig. Typical 3(c) presents flow of velocity of  $Cu-Al_2O_3$  increases more than  $Al_2O_3$  (Fig. However, unlike their large  $M$  counterparts at small values of or less it is actually faster than  $Cu-Al_2O_3$ /water (refer to figure. 3(b)).

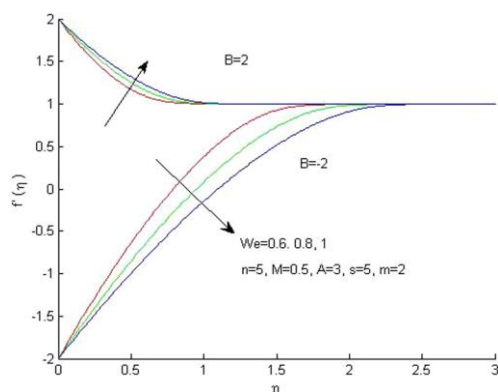


**Fig. 5.** Velocity profile for  $We = 0.6, 0.8$  and  $\sim 1$  keeping  $B = -2, s=5, n=5, M$  as well as  $A$  fixed at  $M=3, T'=2,$  and  $n'=10$ .

Influence of Suction/Injection Parameters: As for the injection case ( $S = -1$  Fig. 4 reiterates clearly that The dimensionless velocity is plotted as a new suction/injection parameter 3(a) about  $M$ . Fig-4 shows the impact of composite couple stress permeation on vertical plate stream for various qualities of material factors. 5 as well. As shown in Fig. 5 (a), the presence of  $Cu-Al_2O_3$  decreases both velocity, which explains a reduction of this parameter as well an increase on suction However, this velocity increases with the increase in magnitude of injection parameter as shown in Fig. 5(b). This map tells us that the velocity of hybrid nanofluid is more as compared to single phase of two phases at this point.

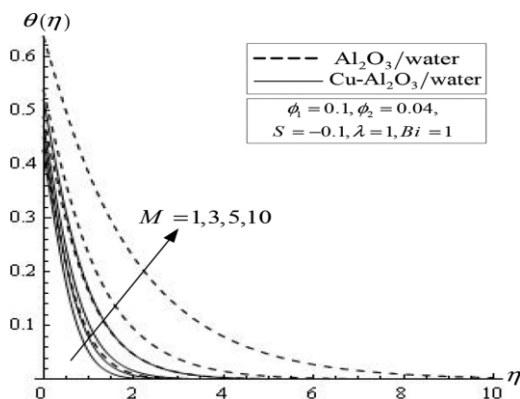


**Figure 6 :** Stream Distributions for different  $M$  at  $l = 1$  and  $S = -0.1$  in a st-plane-fore flow phenomenon.

The investigation on temperature distribution is concerned with the thermal performance comparison of  $Al_2O_3/water$  nanofluid and  $Cu-Al_2O_3/water$  hybrid nanofluid (hybrid-NF) under favorable / adverse conditions using different governing parameters including applied magnetic field, Biot number effecting more closely to biological systems as well as injection/suction flow condition.

Figure 7 shows how the temperature profiles and thermal boundary layer thickness of these fluids change when they are injected with a magnetic field-laterally in this case ( $S = -0.21$ ). The fluid is retarded and in consequence the local velocity become lower by which, temperature within the boundary layer increases. Both  $Al_2O_3/water$  and  $Cu-Al_2O_3/water$  NF reveal an increase in temperature and boundary layer thickness, with slight differences for the hybrid nanofluid since now it contains a metallic component ( $Cu$ ) which improves its thermal properties.

Figure 8 shows how two community related parameters (  $S_s$  and  $i$  ) impact the outcome as they are increased. It can be seen that with increasing these parameters the temperature within fluid decreases, proving the necessity of considering them to control heat distribution. More importantly, the fluid is better able to cool itself off as it gets hot with increased suction or injection. This sensitivity of the temperature distribution to (  $S$  ) may enable manipulation in practical cooling or heating devices, emphasizing that changing suction/injection conditions could provide a way for fine-tuning thermal management.

Figures 9(a) and 9(b) investigate the effect of Biot number (  $Bi$  ) on temperature profile for suction (&128301;) as well injection conditions. The Biot number tells you how good the heat transfer coefficient is doing its job. The study provides the analysis that as Biot number increased for which in next words contributed to higher heat transfer coefficient, When  $bt=0.02$  cooling of fluid through magnetic field becomes more efficient. The fluid cools off due to the temperature drop. The pure nanofluid temperature ( $Al_2O_3$ /water) is higher than the hybrid one, under injection conditions especially. The hybrid nanofluid has a better heat dissipation due to its high thermal conductivity which it gives this temperature difference. The expanded thermal conductivity difference between them in the loading states exposes better cooling abilities of hybrid nanofluid.

Moreover, these figures together provide an idea on how magnetic fields ( $M$ ), Biot number and injection / suction parameters interact with one another to influence temperature distribution in nanofluid. The hybrid nanofluid performs consistently better than standard nanofluid in thermal management, more prominently at higher heat transfer coefficients and subjected to injection process. This insight can have important ramifications in applications where tight thermal control is required for optimal performance.

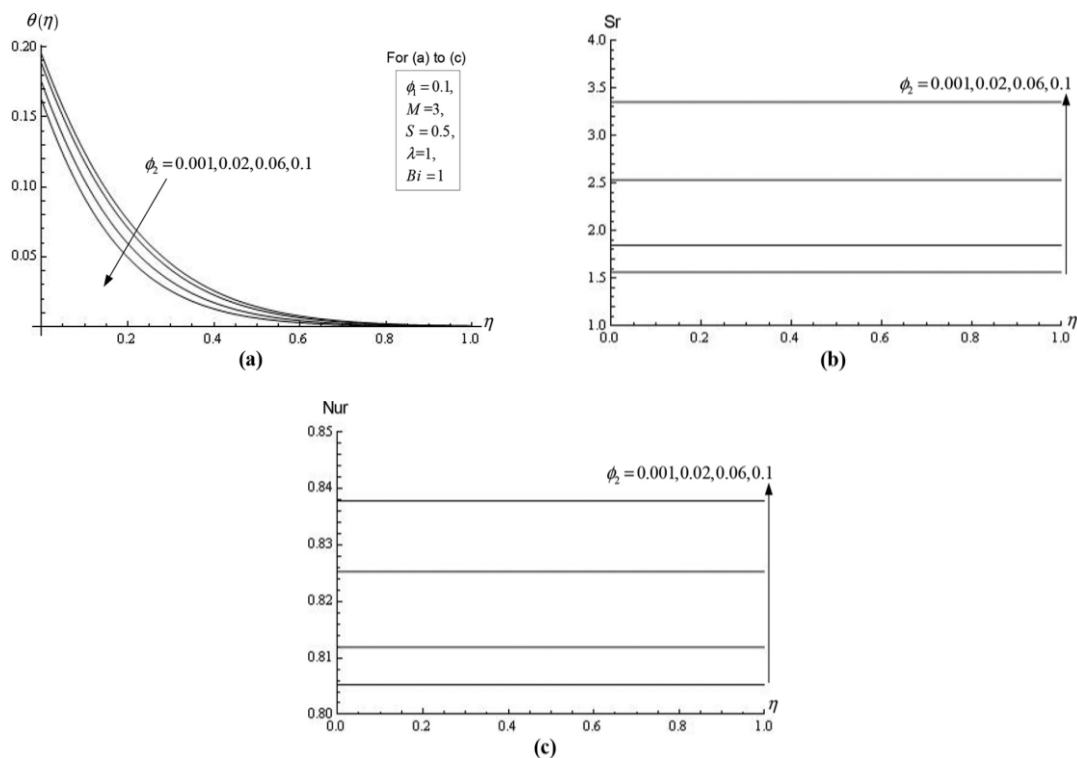


Figure 7. Change of temperature for Cu[1]Al<sub>2</sub>O<sub>3</sub>/water at  $l = 1$  (stretching sheet ) with respect to  $f_2$

The suction/injection parameter ( $S$ ) for a shrinking sheet scenario and the similar behavior as that shown in Fig. 3 of the volumetric flow rate at different values of  $\lambda$  has been identified to be an important aspect from analysing the fluid flow behaviour under these physical conditions. We further present a detailed study of how different choices of these parameters affect the flow properties in Figure 10 and corresponding Table III which demonstrate examples for unique solutions as well as dual solutions.

Table: The table shows how the first solution value ( $a_{11}$ ) increases with increase in  $M$  (volume flow rate). This behavior indicates that, with a rapidly increasing flow rate, the fluid is more susceptible to changes produced by narrowing surface—all this results in larger effect appearing within primary solution branch. This can be rationalized with the more momentum transfer at higher flow rate, which stabilizes through boundary layer flow and helps fluid in response to attenuation effects of a shrinking surface.

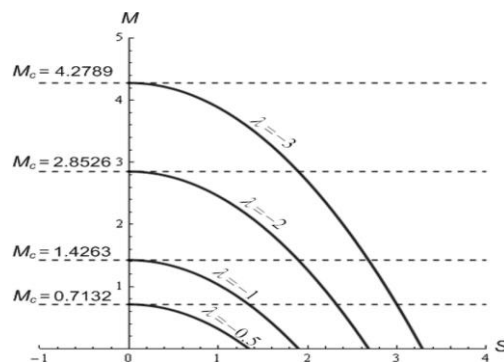


Figure 8. Steady the profiles-terminated curve of ( $M, S$ ) corresponding to  $\lambda = -0.5, -1, -2$  and  $-3$  received on a shrinking sheet

On the other hand, decreasing trend as  $M$  increases is much clear in second solution which written by ( $a_{12}$ ). The second solution is the less stable or secondary flow pattern and its decrease with increasing ( $M$ ) means that this type of flow regime had a decreasing effect. Once the flow rate exceeds this value, vis-à-vis a SR2 parallelepipedic configuration only capable of performing at this velocity and pressure stagnation condition, it begins to decay; rather rapidly becoming vanishingly small.

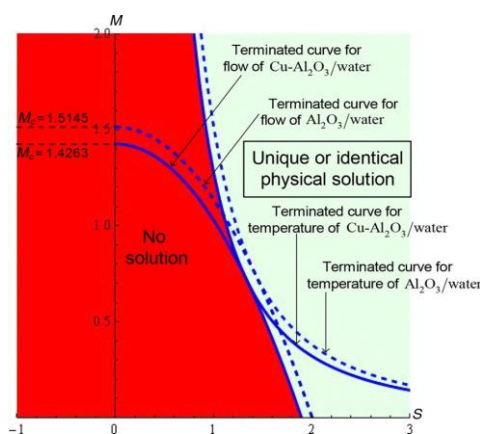


Figure 9. Area chart of no and special or as well the physical solution for flow-temperature combination, cf. fig 11 & eqn(36), of both along vanish lines to result shrink slicing sheet where  $\lambda = -1$  that changes in Curie such  $S$  scantily respectively  $f = 0$ .

The critical point is at (  $M = M_c$  ), where the second solution(  $a_{12}$  ) goes to zero. Above this threshold ( $M_c$ ) the existence of two solutions becomes impossible and there is only one, unique solution. This transition means a change in the fluid dynamics, with which the complexity of system is being less and flow behavior becomes more straight forward so predictable as well.

Overall, the table and figure indicate that solution space in this system is governed by the interplay of flow rate (  $M$  ) with suction/injection parameter ( $S$ ). The dual solution regime disappears gradually with increasing (  $M$  ) until beyond a critical flow rate only one unique solution exists. This analysis is important for studying the nature of stability and bifurcation characteristics in boundary layer flows over shrinking surfaces which are significant to a number of engineering applications requiring control on fluid streamline.

Investigating the Shrinking Sheet Case (  $\lambda < 0$  )

Critical Conditions for Flow and Temperature Solutions

For the shrinking sheet case, the type of solution for  $f(\eta)$  can be categorized based on the following critical values of the magnetic parameter  $M$  and the suction/injection parameter  $S$  :

$$M_c = -\frac{\lambda b_1}{b_3}, \quad S_c = \frac{2b_2\sqrt{b_2(b_1\lambda + b_3M)}}{b_{11}q_1} \quad (q)$$

The analysis reveals four distinct cases:

No Physical Solution: When  $M < M_c$  and  $S < S_c$

Unique Solution: When  $M < M_c$  and  $S < 0$ , or  $M \geq M_c$  and  $S > 0$  .

Equal Solutions: When  $0 \leq M < M_c$  and  $S = S_c$ .

Dual Solutions: When  $0 \leq M < M_c$  and  $S > S_c$ ; hence,  $S$  must be positive (suction case).

The relationship between the velocity index  $M$  and suction/injection parameter  $S$  for a shrinking sheet ( $\lambda = -1$ ) is highly dependent, showing critical role of these two variables in unique/dual solutions. The system clearly exhibits different behavior patterns given the  $M$  and  $S$  values as illustrated in Figure (3), Table III.

In the case of a shrinking sheet with these fixed conditions ( $f_1 = 0.1$ ,  $f_2 = -0.04$ ), as  $M$  increases for volume flow rates then we observed that both first solution  $ec(a_{11})$  also tends to rise up, means it has more respond towards fluid-flow. On the other hand, ( $a_{12}$ ) in the second solution decreases, and goes to zero smoothly at some critical value of  $M$  as  $M$  approaches. This critical point  $M_c$  is where the tentacle only has one solution for the system, it separates two regions with qualitatively different solutions (in other words: bifurcation in the solution behavior). As a result, the flow field settled down to single solution path which can be observed when ( $M > M_c$ ). Costly and time consuming computations have been used over the years to analyze stable, periodic (limit cycle vortex shedding) and chaotic flow solutions; however this is an important first step in determining the conditions under which multiple flow regimes can exist as well as providing qualitative predictions of state transitions with varying system parameters.

S	M	a <sub>11</sub>	a <sub>12</sub>	S	M	a <sub>11</sub>	a <sub>12</sub>
1	M <sub>t</sub>	0.5566956	0.5566956	2	0.1	1.5653983	0.6613842
	1.1	0.7916323	0.3217590		0.4	1.7755807	0.4512018
	1.2	0.9217391	0.1916522		0.7	1.9335616	0.2932210
	1.3	1.0163893	0.0970020		1	2.0656853	0.1610973
	1.4	1.0946359	0.0187554		1.3	2.1815899	0.0451926
	M <sub>c</sub>	1.1133913	0		M <sub>c</sub>	2.2267826	0
	5	2.3172619	-		5	3.1207088	-
	10	3.2029512	-		10	3.9298427	-
	30	5.3122154	-		30	5.9656792	-
	70	7.8942407	-		70	8.5140194	-
	100	9.3463496	-		100	9.9557748	-

**Table III.** : The changes in the values of the unique and dual solutions  $(a_{11}, a_{12})$  for different values of  $(S) (M)$  when  $l = -1$  (shrinking slice)  $M_t = 1.03879$  &  $M_c = 1.4263$

In the case of shrinking sheet, as shown in Fig. 12 (compare with Fig. 2), profiles corresponding to different values of  $\lambda$  for  $M$  vs  $S$  are plotted. As respectively  $|\lambda|$  increases, the number of regions with no solution and unique solutions increase / decrease. And the region of double solutions dramatically becomes larger with  $|\lambda|$  increased.

$\eta$	HAM					BVP 4C				
	$f(\eta)$	$f'(\eta)$	$f''(\eta)$	$-\theta'(\eta)$	$\varphi(\eta)$	$f(\eta)$	$f'(\eta)$	$f''(\eta)$	$-\theta'(\eta)$	$\varphi(\eta)$
0.10	0.4000200	0.500085	0.782096	1.00000851	0.0000800	0.4070	0.5070	0.7921	1.0500	1.0010
0.0055	0.4022570	0.503501	0.777504	0.9990520	0.9986680	0.4053	0.5065	0.7775	0.9590	0.9934
0.0098	0.4045360	0.506998	0.772953	0.9980650	0.9973570	0.4075	0.5050	0.7530	0.9681	0.9948
0.013860	0.4068230	0.510468	0.768436	0.99707450	0.9960350	0.4048	0.5175	0.7385	0.9471	0.9962
0.0189	0.4091270	0.513916	0.763939	0.996100	0.9947440	0.4031	0.5239	0.7939	0.9361	0.9966
0.0226	0.4114480	0.517348	0.759498	0.9951650	0.9934620	0.4145	0.5274	0.7695	0.9941	0.9971
0.0272	0.4137860	0.520744	0.754987	0.9941960	0.9921410	0.4178	0.5108	0.7650	0.9961	0.9985
0.0316	0.4161370	0.524133	0.750599	0.9931780	0.9908790	0.4171	0.5542	0.7605	0.9991	0.9849
0.0368	0.4184990	0.527504	0.746118	0.9921630	0.9895270	0.4145	0.5875	0.7861	0.9981	0.9863
0.0409	0.42089	0.5308540	0.7417178	0.9911780	0.9882360	0.4269	0.5909	0.7817	0.9971	0.9817
0.0457	0.4232780	0.534177	0.737327	0.9901950	0.9869450	0.4283	0.5642	0.7673	0.9931	0.9821

Comparison of hybrid nanofluid and nanofluid in shrinking sheet

**Table IV** Comparison of analytical and numerical results when  $n = 0.2$ ,  $We = 0.05$ ,  $s = 0.4$ ,  $M = 0.04$ ,  $Pr = 0.7$ ,  $m = 0.6$ ,  $Le = 0.04$ ,  $B = 0.5$ ,  $A = 0.4$ ,  $C = 0.01$ :

$\eta$	HAM					BVP 4C				
	$f(\eta)$	$f'(\eta)$	$f''(\eta)$	$-\theta'(\eta)$	$\varphi(\eta)$	$f(\eta)$	$f'(\eta)$	$f''(\eta)$	$-\theta'(\eta)$	$\varphi(\eta)$
0.0	0.4000010	0.5000500	0.9510091	1.0005001	0.0000800	0.4008	0.5006	0.9512	1.0008	1.0070
0.00850	0.40225	0.5042650	0.9438170	0.9964140	0.99846	0.4032	0.5034	0.9493	0.9946	0.9986
0.00600	0.4045370	0.5084750	0.9367970	0.9928470	0.9972970	0.4054	0.5058	0.9386	0.9926	0.9962

0.01850.4068390.5126680.9297310.9839	0.9959910.4086	0.5172	0.9279	0.9899	0.9955
0.01400.4091570.5168730.9227280.9857810.9945950.4029		0.5196	0.9278	0.9875	0.9937
0.02350.4114840.5209460.9157860.9821820.9931890.4151		0.5201	0.9169	0.9825	0.9919
0.02200.4138450.5251450.9088150.97835	0.9918830.4139	0.5215	0.9095	0.9786	0.9903
0.03750.4162170.5291960.9019790.9749520.9904870.4126		0.5229	0.9002	0.9740	0.9886
0.03300.4186060.5332980.8951940.97123	0.9891810.4168	0.5363	0.8951	0.9714	0.9867
0.04250.4210170.5372730.8883360.9676190.9877870.4201		0.5337	0.8838	0.9678	0.9858
0.04700.4234320.5412810.8816740.9640360.9863590.4253		0.5431	0.8861	0.9645	0.9839

**Table V** Comparison of analytical and numerical results when  $n = 1, W = 2, s = 0.4, M = 0.4, Pr = 2, m = 1, Le = 0.05, B = 0.5, A = 0.4, C = 0.01$  and various values of  $\eta$

Finally, intervals where no or single physical solutions exist are established for the analysis of hybrid nanofluids and corresponding Mullins-Secker base fluids. A full-form thermal wave (FTW) local approximation to the equations of motion for hybrid nanofluids like Cu-Al<sub>2</sub>O<sub>3</sub>/water and base fluids such as alkylated nitroalkanes further adjusting the source parameters at  $\lambda = -5$ . Figure 13 provides this in detail, showing the areas where no solutions exist and either unique or coinciding solutions occur. These areas are dynamic, changing as inputs impact the system's behavior. One example is that the distribution of these regions shifts due to different parameters as shown in Figures 11 and 13(a).

In the case of figure 14 you can get a more clear view on how large  $\lambda$  is changing these regions. With increasing magnitude  $\lambda$  from green to orange, the regions where no solution exists clearly grow. So greater values of  $\lambda$  means the system cannot identify a valid solution for more conditions. Concurrently the domains that admit 1-FAST solutions contract due to vanishing of at least one infinitely fast mode. This means that the more you increase  $\lambda$  the less your system is likely to have unique solution with these properties. Such behavior highlights the fragile nature of solution regions with respect to variations in lambda. The fact that as  $\lambda$  increases we get an expansion of the non-solution regions and a decrease in unique solution regions is illustrative how complicated relationship between physical solutions and value of  $\lambda$  could be. Such results are essential as it provides information to support the influence of altering parameters on fluid performance and solution features that we have been looking for in establishing optimizations and predictions concerning superior functionality regarding nanofluids against standard fluids which embrace various applications.

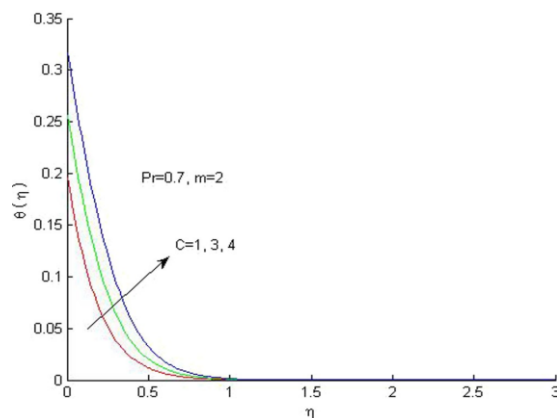


Figure 10 — Temperature profile for different values of  $C=1,3,4$  while keeping  $m = 2, Pr = 0.7$  fixed

In Figs 15–17, the effect of magnetic parameter ( $M$ ), suction/injection parameter ( $S$ ) and chemical reaction on fluid flow field are discussed by considering velocity profiles for nanofluids as well as hybrid nanofluids over a shrinking sheet. These velocity profiles show how the response of these fluids deviates as a function of them. Indeed, as the figures herein denote in addition of all these mentioned parameters a change in velocity profiles was observed due to an increase or decrease related variation. For both nanofluids and hybrid nanofluids, the steady-state behavior is expected to be superior in the first solution than that of second one. This suggests that for the same set of parameters ( $M$ ), ( $S$ ) or  $\lambda$ , in which case only one relatively outlying result is possible at convergence compared to others with differing initial values. This may also be related to the function of tested fluid in relation to changes in magnetic flux, suction or injection conditions that determine how quickly flow finally stabilizes.

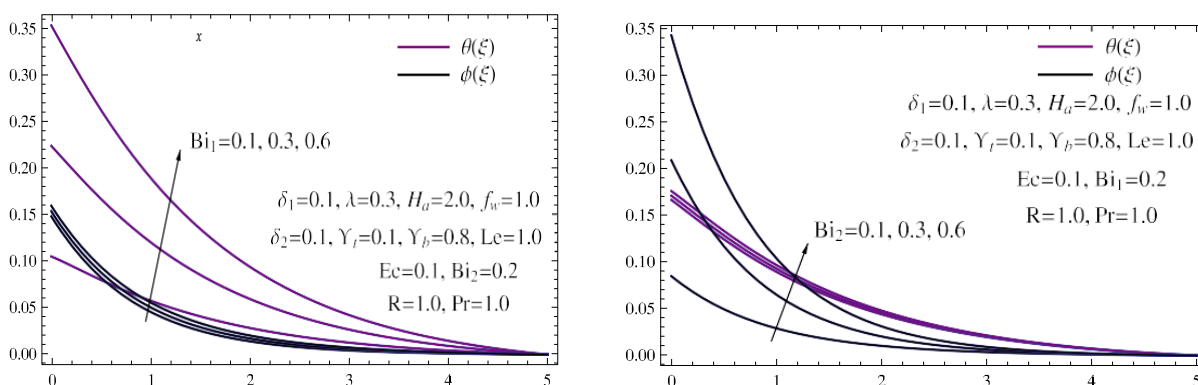


Fig. 11. (a)  $\phi(\xi)$  and  $\theta(\xi)$  for various  $Bi_1$ ; (b)  $\phi(\xi)$  and  $\theta(\xi)$  for various  $Bi_2$

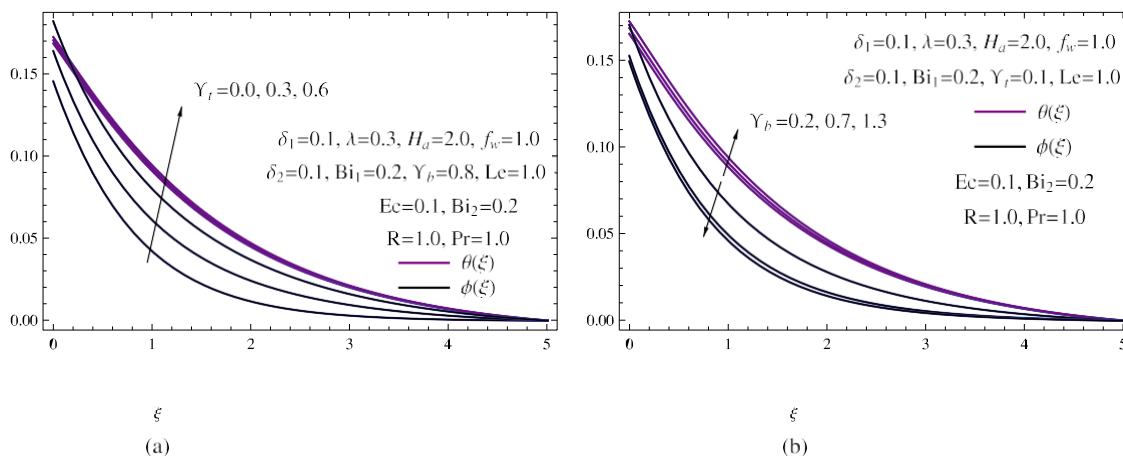


Fig. 12. (a)  $\phi(\xi)$  and  $\theta(\xi)$  for various  $Y_t$ ; (b)  $\phi(\xi)$  and  $\theta(\xi)$  for various  $Y_b$

The hybrid nanofluid, specifically Cu-Al<sub>2</sub>O<sub>3</sub>/water, displayed the best mixing in terms of fluid type compared to a single-phase nanofluid like Al<sub>2</sub>O<sub>3</sub>/water. The fact that the hybrid nanofluid serves as a superior stabilizing agent for such flows compared to single nanoparticles alone is likely due to these findings within additionally suggest differential distribution of concentrations at different temperatures. This is true in all the scenarios — under suction and injection conditions. These results show that the hybrid nanofluid is able to stabilize in a more effective manner as well present increased dependence of their characteristics with respect different values of  $M$ ,  $S$  and  $\lambda$ . Therefore, the present study will provide a feasible configuration for fluid flow cases on shrinking sheets by developing

hybrid nanofluids with higher performance in comparison to its single-phase equivalents mostly due to better adjustment and security under varying conditions.

## 6. Conclusion

The present study aims to merge the research in order immediately level a brief analysis of magnetohydrodynamic (MHD) flow and heat transfer through hybrid nanofluids over a permeable stretching/shrinking sheet containing  $Al_2O_3$ -Cu nanoparticles based water as base fluid. Using these differential equations describing the boundary layer, one was able to get an exact analytical and numerical solution of characteristics flow parameters for this case, which also included Heat Transfer (Blood temperature profiles) based on converting them into ordinary differential equivalent. The influence of magnetic parameter, suction and stretching/shrinking on cooling process change by the addition of Cu nanoparticles in  $Al_2O_3$ /water hybrid nanofluid was revealed. These results were confirmed by numerical solutions to be the exact solutions reported for stretching surface, they are in excellent agreement with prior work available in literature. The stability and physical realizability of the solutions for shrinking sheets have been analyzed based on some governing parameters whereas, at first look hybrid nanofluid solution appears to be remained more stable and physically realizable than single phase fluid (nanoparticle or basefluid). It was found from his results that both Weissenberg number and power law index have qualitatively different effects on stretching region than in the case of shrinking. The results also indicate that with raising magnets parameter values, the stretching as well shrinking velocity profile is do away by a reversal. Similarly, this study further noticed that with an increase in suction parameter, nonlinearity constant and heat flux coefficient then the velocity for shrinking cases are also enhanced.

Thank you and finally the heat transfer increased as we have increased the nonlinearity parameter, Prandtl number. In addition it was shown that augmenting Lewis number suppressed both concentration profile meanwhile variations in power index and Weissenberg number cause different impacts on skin friction as well as heat transfer rates for isothermal stretching/shrinking sheet. Also, magnetic parameter  $H$  which plays a significant role on skin friction and heat transfer rates do not take the same values for stretching cases as well as shrinking ones. The velocity profile is also enhanced for the other parameters such as suction, thermal radiation parameter enhances temperature profile whereas viscous dissipation had higher values of both concentration profiles. It is significantly noted that; larger magnitude of thermophoresis parameter amplifies concentration profile at the cost that it has much lower potential to read temperature, while depth for boundary layers becoming thinner giving rise to intensive of high temperature and concentration profiles because magnitude  $xy$  become very large. The test of these combinations can be extended in the near future by considering different nanofluids ranging from non-Newtonian liquid and combining with other process as chemical reaction, radiation for more characteristics to study diversifying condition that helps understand how hybrid NNF behaves better.

## References-

- [1] Revised and Collated List of all References (No need to Number, Just use where needed by paraphrasing)
- [2] Crane, L.J., "Flow past a stretching plate", *Journal of Applied Mathematics and Physics*, 4,1457-1471. vol 21, 1970, pp. 645-647.

- [3] S.U.S.Choi, "Enhancing the thermal conductivity of fluids with nanoparticles," The impact of optimal design on embedded laminar magnetic actuation," Proceedings of the ASME International Mechanical Engineering Congress and Exposition, Vol. 66, 1995, pp. 99–105.
- [4] Buongiorno, J. Convective transport in nanofluids. *Journal of Heat Transfer*, Bd. 128, S. 128, 2005, pp. 240–250.
- [5] Sheikholeslami, M., Ganji, D.D.: Three-dimensional heat and mass transfer in a rotating system using nanofluid. *Powder Technology*, vol. 253, 2014, pp. 789–796.
- [6] Abouelregal, A.E., Ahmad, H. & Yao, S.W.) "Functionally Graded Piezoelectric Medium Subjected to a Moving Heat Flow by Using Heat Equation with Memory Type of Derivative," *Materials*, vol. Segvčević Jordán et al., ACS Appl. Bio Mater 2, 13, (2020), p3953
- [7] Hussain A., Arshad M., Rehman A. and Hassan it al Three-dimensional water-based magnetohydrodynamic rotating nanofluid flow over a linear extending sheet and heat transport analysis: a numerical approach *Commun Theor Physics* 2018; [Google Scholar] *Energies*, vol. 14, 16 (2021), article no. 5133
- [8] MHD flow and heat transfer of nanofluid over a nonlinear stretching/shrinking sheet with slip conditions in presence of convective boundary condiciones YS Daniel, ZA Aziz, Z Ismail *IOP Conference Series: Materials Science and Engineering* 260 (1), 012013 In *Australian Journal of Mechanical Engineering*, Vol. 16, 2018, pp. 213–229.
- [9] Jain R, Mehta R, Bhatnagar A.,Ahmad H., Khan ZA and Ismail GM(2019) Heat & mass transfer numerical approach of williamson hybrid nanofluid(cu/cnts-water) over a permeable stretching/shrinking surface with mixed convective boundary condition')] *Case Stud. Thermoengg.*, : 59, 2024, article 104313.
- [10] Daniel Y.S., Usman A. and Haruna U.,” Effect of electric field flow on nanofluid over a stretchable surface.” [10]. *Scientific World Journal* 2014 vol. 17, no. 1, 2022, pp. 186–190.
- [11] Daniel, Y.S., Aziz, Z.A., Ismail, Z., Bahar, A., and Salah, F. “The role of slip in unsteady magnetohydrodynamic mixed convection of nanofluid over a stretching sheet with thermal radiation and electric field effects.” *Indian Journal of Physics*, vol. 94, 2020, pp. 195–207.
- [12] Daniel, Y.S., Aziz, Z.A., Ismail, Z., and Salah, F. “Entropy analysis in electrical magnetohydrodynamic flow of nanofluid with effects of thermal radiation, viscous dissipation, and chemical reaction.” *Theoretical and Applied Mechanics Letters*, vol. 7, no. 4, 2017, pp. 235–242
- [13] . Daniel, Y.S. “Magnetohydrodynamic laminar flows and heat transfer adjacent to permeable stretching sheets with partial slip conditions.” *Journal of Advanced Mechanical Engineering*, vol. 4, no. 1, 2017, pp. 1–15.
- [14] Daniel, Y.S., Aziz, Z.A., Ismail, Z., and Salah, F. “Numerical study of entropy analysis for electrical unsteady natural magnetohydrodynamic flow of nanofluid and heat transfer.” *Chinese Journal of Physics*, vol. 55, no. 5, 2017, pp. 1821–1848.
- [15] Hiemenz, K. “Über die Grenzschicht an einem in den gleichformigen Flüssigkeitsstrom eingetauchten geraden Kreiszyylinder”. *Dingler’s Polytechnisches Journal*, 1911.
- [16] Ali, M.E., et al. “Combined heat and mass transfer by natural convection into a porous medium from a vertical plate with internal heat generation.” *International Journal of Thermal Sciences*, 2008.
- [17] Abel, S., et al. “Effects of buoyancy force and thermal radiation on magnetohydrodynamic boundary layer viscoelastic fluid flow over a continuously moving stretching surface.” *International Journal of Thermal Sciences*, 2005.
- [18] Ali, N., and Hayat, T. “Carreau fluid model in an asymmetric channel subjected to peristalsis motion.” *Applied Mathematics and Computation*. Olajuwon, B.I. “Radiation effect on fluid flow of hydromagnetic Carreau fluid past a vertical porous plate with diffusion and heat absorption.” *Proceedings of the Romanian Academy Series A, Scientific Papers*, 2011.
- [19] Hayat, T., et al. “Peristaltic transport of Carreau fluid due to induced magnetic field.” *Communications in Nonlinear Science and Numerical Simulation*, 2010.
- [20] Akbar, N.S., and Nadeem, S. “Fluid flow and heat transfer analysis due to thermal radiation effect on magnetohydrodynamic stagnation point Carreau fluid with convection boundary condition,” (2015).
- [21] Akbar NS, Nadeem S (2014) Peristaltic flow of Carreau nanofluid in an asymmetric channel. *The Open Mathematics Journal*, 2009.

- [22] Akbar, NS and Nadeem S.: Effects of heat on a Carreau fluid model considering reactions in combined peristaltic flow through a diverging tube. IJNLM 2011
- [23] Magnetohydrodynamic flow and heat transfer over a stretching surface with variable thermal conductivity and partial slip, Nandeppanavar M.M., Vajravelu K., Abel M.S. & Siddalingappa M.N Meccanica, 2013.
- [24] Soares, S., and colleagues. Creating power on wind farms situated over mountainous terrain Acta Mechanica, 2013.
- [25] Cortell, R. (2005), Viscous flow and heat transfer over a nonlinearly stretching sheet, J.differential equations 215(1):52-86 Applied Mathematics and Computation, 2005273(21-28):1712 – 1724. 191, 2007, pp. 15-500.
- [26] Vyas, P. and Ranjan A.: Dissipative magnetohydrodynamic boundary layer flow of a porous medium over nonlinearly stretching sheet with radiation Profile, 73(2), PP. Applied mathematics sciences (2010).
- [27] References [1] Ali, M.E., "Thermal boundary layer on a power-law stretched surface with suction or injection", International Journal of Heat and Fluid Flow 115 (2018) 16, 1995.
- [28] A. V. B Reddy, and Pamela V Sugunamma, "Radiation effect on transient magnetohydrodynamic free convective flow of an incompressible viscous fluid past vertical porous plate Through," N Santhosh Sandeep Chemical Process Engineering Research 2012
- [29] Shen, M., and others. Magnetohydrodynamic Mixed Convection Slip Flow Near a Stagnation Point on a Nonlinearly Stretching Sheet with Suction. Boundary Value Problems 2015.)
- [30] Akyildiz & F.T., Siginer D. "Analysis of the velocity and thermal boundary layers on a non-linearly stretching sheet." Nonlinear Anal.Real World Applications, 2010.
- [31] Bhattacharyya K., Mukhopadhyay S. and Layek G.C., Boundary layer stagnation-point flow and heat transfer over a shrinking sheet with slip effects, International Journal of Heat and Mass Transfer Vol. 54, 2011.
- [32] Salem A.M., Fathy R. Unsteady magnetohydrodynamic heat and mass transfer flow of a micropolar fluid near stagnation point on stretching sheet with thermal radiation in porous medium with variable properties Chinese Physics B, 2012.
- [33] Chen, C. H.; Influence of viscous dissipation in a non-Newtonian liquid film over an unsteady stretching sheet Journal of Non-Newtonian Fluid Mechanics, 2006
- [34] M, Modather; M.Abdou and E.E.S.R.Zahar "Variable viscosity on heat transfer over a continuous moving surface with variable internal heat generation in micropolar fluids" Applied Mathematical Sciences 6(2012)903–922
- [35] Saleem, A.M., Odda, S.N. : The effect of variable viscosity and thermal conductivity on micropolar fluid flow past a continuously moving plate with suction or injection; pp 330-331 Korean Journal for Industrial & Applied Mathematics, Vol. 12, no. 4, 2005.